Clinical Pharmacokinetics (2025) 64:715–728
https://doi.org/10.1007/s40262-025-01504-5

ORIGINAL RESEARCH ARTICLE

Model-Informed Dose Optimization of Pazopanib in Real-World Patients with Cancer

Zhiyuan Tan[1,2] · Swantje Völler[1] · Anyue Yin[2] · Amy Rieborn[2,3] · Hans Gelderblom[3] · Tom van der Hulle[3] · Catherijne A. J. Knibbe[1,4] · Dirk Jan A. R. Moes[2]

Accepted: 24 March 2025 / Published online: 22 April 2025

Abstract

Background and Objectives Pazopanib is approved for metastatic renal cell carcinoma (mRCC) and soft tissue sarcoma (STS) in a dose of 800 mg once daily (QD) taken under fasted conditions. In clinical practice, approximately 60% of patients require dose reductions due to toxicity, with severe liver toxicity necessitating treatment interruptions in over 10% of cases. While a trough concentration ($C_{min,ss}$) target of ≥ 20.5 mg/L has been established for mRCC efficacy, no specific threshold exists for liver toxicity. The objectives of this study were to develop a population pharmacokinetic (POPPK), an exposure–liver toxicity, and an exposure–tumor size dynamics model to optimize pazopanib initial dose in real-world patients.

Methods In total, 135 patients were included and treated with a median starting dose of 800 mg (interquartile range, IQR: 600–800 mg) QD pazopanib fasted with a median follow-up of 120 (IQR 63–372) days. A population pharmacokinetic model was developed using 460 concentration measurements from 135 patients. Exposure–liver toxicity was evaluated using time-to-event modeling, and exposure–tumor size dynamics was evaluated using tumor growth modelling.

Results The liver toxicity model, with 27 cases of grade ≥ 2 liver toxicity out of 135 patients (20%), identified a $C_{min,ss}$ threshold of > 34 mg/L associated with a 3.35-fold increased toxicity risk ($P < 0.01$). Model simulations showed that an initial dose of 600 mg QD significantly reduced liver toxicity risk ($P < 0.001$) while maintaining $C_{min,ss}$ ≥ 20.5 mg/L for 76% of the simulated individuals. Tumor size dynamics were analyzed using baseline and posttreatment tumor size measurements from 111 patients. The introduction of primary resistance by using a mixture model improved the model fit significantly. Tumor growth and decay rates differed between mRCC and STS but showed no pazopanib exposure dependency across the studied range, suggesting maximal tumor inhibition at current exposure levels.

Conclusions These findings suggest that an initial pazopanib dose of 600 mg fasted, followed by model-informed precision dosing to maintain $C_{min,ss}$ between 20 and 34 mg/L, may improve efficacy–toxicity balance and mitigate treatment interruptions.

1 Introduction

Pazopanib is a tyrosine kinase inhibitor (TKI) against vascular endothelial growth factor receptor (VEGFR) [1]. In 2009, it was approved for the treatment of patients with metastatic renal cell carcinoma (mRCC) [2]. To date, several guidelines recommend pazopanib for use as single agent or combined with programmed cell death protein 1 (PD− 1) inhibitors in first-line treatment for mRCC [3, 4]. In 2012, it was also approved for patients with advanced soft tissue sarcoma (STS) who received prior chemotherapy [5].

A fixed 800 mg fasted daily dose is the registered dose that is recommended for all patients, regardless of tumor type [6]. It has been suggested that the efficacy of pazopanib

✉ Dirk Jan A. R. Moes
d.j.a.r.moes@lumc.nl

1 Division of Systems Pharmacology and Pharmacy, Leiden Academic Center for Drug Research, Leiden University, Leiden, The Netherlands

2 Department of Clinical Pharmacy & Toxicology, Leiden University Medical Center, Albinusdreef 2, 2333 ZA Leiden, The Netherlands

3 Department of Medical Oncology, Leiden University Medical Center, Leiden, The Netherlands

4 Department of Clinical Pharmacy, St Antonius Hospital, Nieuwegein, The Netherlands

Key Points

A steady-state minimum concentration ($C_{min,ss}$) > 34 mg/L predicts increased risk of pazopanib Common Terminology Criteria for Adverse Events (CTCAE) grade ≥ 2 liver toxicity in patients with metastatic renal cell carcinoma (mRCC) and soft tissue sarcoma (STS).

No significant relationship was found between pazopanib exposure levels and tumor size dynamics in real-world mRCC and STS patient populations.

Initiating pazopanib at 600 mg once daily fasted significantly reduces the risk of liver toxicity while maintaining therapeutic efficacy. Targeting a $C_{min,ss}$ range of 20–34 mg/L may enhance treatment outcomes and minimize adverse effects, supporting optimized dosing strategies in clinical practice.

is related to the steady-state trough concentration ($C_{min,ss}$). A $C_{min,ss} \geq 20.5$ mg/L was associated with improved progression-free survival (PFS; i.e., 19.6 versus 52.0 weeks, $p = 0.004$) and tumor shrinkage in a retrospective analysis in 177 patients with mRCC [7]. Therefore, a newly published therapeutic drug monitoring (TDM) guideline [8] recommends that pazopanib dose selection should be supported by model-informed precision dosing (MIPD), targeting plasma $C_{min,ss} \geq 20.5$ mg/L [7]. However, there is no information about the target $C_{min,ss}$ in patients with STS, nor about the thresholds for toxicity of pazopanib.

In a renal cell carcinoma patient population, the incidence of increased mean arterial blood pressure (MAP), diarrhea, hair color change, alanine aminotransferase (ALT) increase, stomatitis, and hand-foot syndrome increased as the plasma pazopanib concentrations increased, with the highest incidence occurring in the fourth $C_{min,ss}$ quartile [7]. Among these toxicities, the most common adverse events related to pazopanib are liver toxicities such as aspartate transaminase (AST) and ALT elevations [9], which lead to dose reductions for mild elevations and to drug discontinuation for severe elevations. In the pazopanib drug label, liver toxicity was emphasized with a black box warning because around 60% of the patients included in the registration study developed liver toxicity and 12% of the patients experienced severe liver enzyme elevations [10]. A similar incidence was also observed in real-world practice, where 40–60% of the patients experienced liver toxicity when treated with pazopanib [11]. So far, only a correlation of Common Terminology Criteria for Adverse Events (CTCAE) grade ≥ 3 overall toxicity, which is also phrased as severe toxicity, and pazopanib exposure was established for patients with mRCC, which is $C_{min,ss}$ < 46–50 mg/L [12, 13].

MIPD is a concept that employs mathematical models to design personalized dosing strategies [14]. The benefit of MIPD for targeted therapy has been confirmed by different studies [15, 16], while no study for pazopanib has been reported yet. Therefore, the objectives of this study are to: (i) develop a population pharmacokinetics (POPPK) model using drug concentrations obtained during TDM in real-world practice; (ii) explore the pazopanib exposure–liver toxicity relationship in patients with RCC and patients with STS; and (iii) explore the pazopanib exposure–tumor size relationship for the two tumor types. Ultimately, these efforts will result in an optimized initial dose of pazopanib, resulting in optimal efficacy–safety balance.

2 Methods

2.1 Patients and Data Collection

2.1.1 PK Data

Pazopanib plasma concentration measurements were obtained from patients diagnosed with mRCC or STS who received treatment at Leiden University Medical Center (LUMC) between February 2014 and July 2022. These data were identified from the hospital electronic patient dossier system (HiX, Chipsoft B.V. Amsterdam) and retrieved using the Clinical Data Collector tool (CTcue; v3.1.0, CTcue B.V., Amsterdam, The Netherlands). The bioanalytical assay used was a validated liquid chromatography–mass spectrometry method according to the European Medicines Agency (EMA) guidelines with a precision (coefficient of variation, CV%) of 2.4% and an accuracy of 11% [17]. Patients needed to have at least one pazopanib PK measurement during the treatment. Samples with time after the last pazopanib intake (TAD) between 20 and 28 h were defined as trough concentration. Patients' demographic information, including age, sex, body mass index (BMI), weight, height, and tumor type, was also collected for covariate analysis. A TDM routine was performed for each individual, and the dose-adjustment algorithm is depicted in Supplementary Fig. S1.

2.1.2 Liver Toxicity Data

The laboratory assessment data was obtained with CTcue and consists of the relevant liver enzymes ALT, AST, and alkaline phosphatase (ALP). These laboratory assessment data were extracted for the included patients between their start and end day of pazopanib use. Toxicity event was

defined as CTCAE (V5.0) [18] grade ≥ 2 ALT or AST or ALP elevation.

2.1.3 Tumor Size Data

Tumor size was defined as the sum of longest diameter (SLD) of target lesions, using RECIST 1.1 criteria [19]. Individual lesions records were retrieved from computed tomography (CT) scans in the electronic patient dossier. Patients who did not have available baseline tumor size data were excluded.

This study was conducted in accordance with Good Clinical Practice guidelines and the Declaration of Helsinki. The protocol was approved by the institutional review board (IRB) at Scientific Committee of Clinical Oncology, Medical Ethics Review Committee Leiden/Den Haag/Delft (approval number: G21.200). As data from routine care were used, a waiver was granted for the requirement of informed consent by IRB.

2.2 Population Pharmacokinetics Analysis

Using pazopanib concentration versus time after dose data, a POPPK model was developed to describe the PK profiles of the included patients. The study first explored both one- and two-compartment models with first-order oral absorption. Given the known dose-dependent, nonlinear absorption characteristics of pazopanib tablets, besides linear absorption, an additional published dual absorption rate (Ka) model, accounting for dose- and time-dependent bioavailability (F_1), was evaluated (Yu et al. [20]) by fixing to the published values. In addition, other potential nonlinear apparent clearance (CL/F) models were also evaluated. The influence of disease types on the CL/F of pazopanib was also examined. All PK parameters were assumed to follow a log-normal distribution, and interindividual variability (IIV) was incorporated into different PK parameters as shown in Eq. (1):

$$P_i = P \times e^{(\eta_i, \mathrm{IIV})} \tag{1}$$

where P_i represents the individual PK parameter estimates, P denotes the typical population parameter estimate, and $\eta_{i,\mathrm{IIV}}$ represents the random IIV which was assumed to follow a normal distribution with a mean of 0 and a variance of ω [2]. The residual error was characterized with a proportional model, an additive model, or a combined proportional and additive model.

After the structural model was determined, different covariate effects on CL/F and volume of distribution (V/F) were investigated with a stepwise covariate modeling (SCM) algorithm, which is a built-in function of Perl-speaks-NONMEM (PsN, version 5.3.1). The evaluated covariates included concomitant medication tumor type, food effect, age, sex, body weight, and BMI. Since pazopanib is a substrate of CYP3 A4, concomitant medication use of CYP3 A4 inhibitors and inducers was also evaluated next to gastric acid-suppressive agents [21]. Model selection was based on the change in objective function value (dOFV). The *P*-values were set as 0.05 (dOFV ≥ 3.84 for 1 or more degrees of freedom) for the forward selection and 0.01 (dOFV ≥ 6.64 for 1 or more degrees of freedom) for the backward elimination process.

Goodness-of-fit (GOF) plots were used to evaluate the fit of the studied models. GOF plots were stratified by tumor types to investigate potential differences between mRCC and STS patients. Bootstraps were used to evaluate model estimation uncertainty. Simulation-based evaluation was carried out with a prediction-corrected visual predictive check (pcVPC) [22].

2.3 Exposure–Liver Toxicity Analysis

A nonparametric Kaplan–Meier plot divided by tumor type was first derived to compare the difference between mRCC and STS. Then, a time-to-first-event (TTE) modeling approach was used to explore the hazard of occurrence of CTCAE ≥ 2 liver toxicity between the start of the pazopanib treatment and the last available laboratory investigation records before the end of pazopanib treatment or before the follow-up time ended (censored time was set to 365 days after the initiation of pazopanib treatment). For parametric TTE modeling, the likelihood of the binary event data given the survival function was calculated according to Eqs. 2 and 3.

$$S(t) = e^{-\mathrm{cumhaz}} \tag{2}$$

$$\mathrm{cumhaz} = \int_0^{\mathrm{t}} h(t)\mathrm{d}t \tag{3}$$

where $S(t)$ denotes the time course of the probability of survival, cumhaz represents the cumulative hazard between the time of follow-up start and the time t (the time of the event or the time of censoring) and $h(t)$ represents the hazard of an individual subject at the time of the event.

In total, five basic hazard models were evaluated for the TTE model development, namely Weibull, exponential, gompertz, log-logistic, and log-normal models [23]. The hazard model that best fit our data was selected on the basis of the change of OFV and survival-based visual predictive check (sVPC). In addition, a hazard-based VPC (hVPC) adapted from a previously established algorithm and R package [24] was created to assist the evaluation of hazard function.

The established pazopanib POPPK model was used to generate pazopanib exposure over time for all included patients, including $C_{min,ss}$ (the trough concentration on the day of the toxicity event or the day of the censoring), maximum concentration C_{max} (the maximum concentration on the day of the toxicity event or the day of the censoring), area under the curve every 24 h ($AUC_{24\,h}$, on the day of the toxicity event or the day of the censoring). The effects of exposure metrics $C_{min,ss}$, C_{max}, and $AUC_{24\,h}$ (following equations will use $EXPOSURE_{pazo}$ to represent the exposure metrics of pazopanib) were evaluated with a linear and an exponential function (Eqs. 4 and 5), where $h(t)$ represents the hazard at the specific time point, $h(t)_0$ represents the base hazard at the start of the pazopanib treatment, and $EXPOSURE_{pazo}$ represents the effect of the pazopanib exposure metrics. A decrease of more than 3.84 in OFV ($P < 0.05$) after adding $EXPOSURE_{pazo}$ compared with the basic TTE model was considered to suggest a significant effect of exposure metrics on the hazard of liver toxicity occurrence. Finally, a toxicity cutoff target was determined by evaluating different concentrations as a threshold. For this purpose, Eq. 6 was applied, and θ was estimated if the pazopanib concentration was higher than the XX mg/L (or mg*h/L) threshold. In addition to $EXPOSURE_{pazo}$, other covariates including pazopanib dose just before the toxicity event, pazopanib initial dose, age, body weight, sex and tumor type were also evaluated.

$$h(t) = h(t)_0 \times (1 + \theta \times \text{EXPOSUREpazo}) \tag{4}$$

$$h(t) = h(t)_0 \times e^{(\theta \times \text{EXPOSUREpazo})} \tag{5}$$

$$\text{If EXPOUSREpazo} > \text{XX}, h(t) = h(t)_0 \times e^{(\theta \times \text{EXPOSUREpazo})} \tag{6}$$

2.4 Exposure–Tumor Size Dynamics Analysis

Exposure–tumor size dynamics analysis using the sum of longest diameter of target lesions (SLD, in mm) after and during pazopanib as response endpoint was performed. The population was assumed to consist of two subpopulations at the start of treatment: a pazopanib primary sensitive population (SLD_s) and a pazopanib primary resistant population (SLD_r) for which a mixture model was used. The structural model development strategy was: (1) determine a semi-mechanistic model with apparent growth rate (KG), apparent decay rate (KD), and acquired resistance (λ); (2) implement a mixture model to identify patients with primary resistance; (3) investigate the effect of exposure ($EXPOSURE_{pazo}$, same exposure metrics as in toxicity analysis) on tumor growth and (4) perform a covariates analysis on the established model. The mRCC and STS population were first modeled together, and tumor type was used as a covariate. Later, standalone models for both diseases were also developed separately. Owing to the sparse tumor size data in the STS population, the baseline tumor size was used as input variable instead of estimating it to improve the stability of the model.

After the mixture model for SLD_s and SLD_r subpopulations was established, pazopanib time-varying exposure metrics derived from the PK model, including the trough concentration of each day of treatment, C_{max}, and AUC24, were added to the model (step (3)). KD was assumed to depend on pazopanib exposure, and linear, exponential, and Emax relationships were tested separately to select the best equation.

Finally, the IIVs of parameters were evaluated, and parameters were assumed to be log-normally distributed. The combined proportional and additive model was applied to characterize the residual error. The model fit was evaluated by dOFV, GOF plots, and pcVPC, considering the censoring of data.

2.5 Model-Based Simulations for Treatment Optimization

On the basis of the final pazopanib POPPK model, liver toxicity model, and tumor size dynamics model, simulations were performed to optimize the starting dose. A total of three dose regimens—800 mg once daily (QD), 600 mg QD, and 400 mg QD—were compared in the simulations. In total, 1000 simulations for each regimen were performed over a follow-up period of 365 days after treatment initiation. Median pazopanib concentration and 90% prediction intervals were plotted to visualize the exposure over time. Additionally, the median probability of developing CTCAE $\geq$ 2 liver toxicity with 95% confidence intervals were included. Median tumor size over time with 90% prediction intervals was visualized separately for mRCC and STS populations to represent the differences in response between the two tumor types.

Additionally, using the final POPPK model, a shiny application was created on the basis of the shiny package (version 1.9.1) and the mapbayr package [25] in R (The R Foundation for Statistical Computing) to perform maximum a posterior Bayesian estimation for a random patient with a random measured concentration and to provide dose adjustment recommendations on the basis of the individual parameter and simulations.

2.6 Software and Estimation Methods

The population PK and PK/pharmacodynamics (PD) modeling analyses in this study were performed with NONMEM (version 7.4.4, ICON Development Solutions). The

first-order conditional estimation with interaction (FOCE-I) algorithm was selected as the parameter estimation method for POPPK and tumor size modeling. The first-order (FO) algorithm was selected as likelihood estimation method for toxicity analysis. Data management, data formatting, results visualization, and basic statistical analysis were performed with R statistics software (version 4.2.1).

3 Results

3.1 Patients and Data

In this model-based analysis, 132 patients were included with a histology diagnosis of mRCC ($n = 93$) or STS ($n = 39$) who received pazopanib treatment from January 2014 to January 2023 at LUMC. Patients who interrupted the pazopanib for more than 6 months were treated as two different individuals, and therefore, the final dataset included 135 patients of which 96 (71%) were patients with mRCC. Both patients with mRCC and patients with STS were initiated at a median dose of 800 mg (interquartile range, IQR: 600–800 mg) QD, and used a median dose of 600 mg (IQR 400–800 mg) QD during the pazopanib treatment, as depicted in Table 1.

For the pazopanib PK measurements, in total, 460 samples were included, of which 70% were trough concentrations. The median time after dose was 24 h with a range of 0.5–166 h. The median observed pazopanib concentration was 28 mg/L for mRCC and 30 mg/L for STS. Median individual predicted $C_{min,ss}$ was 27 mg/L (IQR 22–35 mg/L) for both tumor types generated by the POPPK model, described in Table 2. None of the collected concentrations were below the lower limit of quantification [17]. The collected observations over time after dose are shown in Supplementary Fig. S2.

The laboratory assessment data representing the liver function during pazopanib treatment of all included 135 patients were available for toxicity analysis. A total of 27 out of 135 patients (20%) experienced an CTCAE ≥ 2 elevated ALT, AST, or ALP within 1 year censoring time after treatment initiation. Regarding tumor size, which was expressed as SLD, of the studied population, 24 patients either did not have a traceable baseline SLD or did not undergo a CT scan during pazopanib treatment and were therefore excluded from the cohort for tumor size dynamics analysis. Baseline median SLD of mRCC was 79 (IQR 50–129) mm, and STS was 88 (64–148) mm. During the pazopanib treatment, the median SLD of patients with mRCC was 53 (IQR 33–103) mm, while that of the patients with STS was 112 (IQR 61–160) mm. The baseline patient demographics, disease characteristics, dosing information, and tumor size data information of the included patients are summarized in Table 1.

3.2 POPPK Model of Pazopanib

A one-compartment POPPK model with first-order elimination, linear absorption, and dose-nonlinearity on bioavailability (F_1) was established with the available pazopanib PK data. Owing to the limited data in the absorption phase, Ka was fixed to the reported value [26] as this model was also based on a population that from real-world practice [26]. F_1 was fixed to 1, and IIV of CL/F, V/F and F_1 were estimated, resulting in improved model fit. Compared with constant F1, dose-nonlinearity significantly improved the model performance, empirical Bayesian estimates (EBE) distribution, and OFV. None of the tested covariates (tumor type, age, body weight, or sex) significantly influenced any of the PK parameters. Concomitant use of CYP3 A4 inhibitors and inducers was not observed in our cohort. The parameter estimates of the final pazopanib POPPK model are presented in Table 2. The relative standard errors (RSEs) were less than 20% for all typical values and slightly higher for IIV of V/F (57%). Bootstrap results indicated a stable estimation, as presented in the last column of Table 2.

The GOF plots of the final pazopanib PK model demonstrated an adequate description of observations by both individual predictions (IPRED) and population predictions (PRED), as shown in Supplementary Fig. S3. The conditional weighted residual errors (CWRES) were randomly distributed around zero without obvious trends over population predictions or TAD. pcVPC of 1000 simulations indicated a good description of the model to the data, as shown in Supplementary Fig. S4a. Dose linearity was also depicted in Supplementary Fig. S4 (b).

3.3 Exposure–Liver Toxicity Analysis

The raw data visualization of the percentage change of liver enzyme (yellow line) over time and pazopanib-predicted $C_{min,ss}$ over time (dashed black line) after pazopanib treatment initiation of each individual are provided in Supplementary Fig. S5. The nonparametric Kaplan–Meier analysis of observed events of CTCAE ≥ 2 liver toxicity and censored data with confidence intervals is depicted in Supplementary Fig. S6. This shows that there is no significant difference in the development of a liver toxicity event between patients with mRCC and patients with STS, while higher $C_{min,ss}$ (≥ 34 mg/L) significantly differs from the lower $C_{min,ss}$ group (< 34 mg/L). A gompertz model was selected as the base model, with a significantly lower OFV (dOFV > 20) than the other models, and it described the data well.

Table 1 Baseline patient demographics, disease characteristics, dosing information, and tumor size data information from the included patients with mRCC and patients with STS in the analysis

Parameters	Total	mRCC	STS
Patient characteristics			
Total number of patients (*N*, %)	135	96 (71%)	39 (29%)
Male/female (%male of total)	85/50 (63%)	69/30 (72%)	16/23 (41%)
Age (years, median [range])	67 [21–89]	69 [48–89]	51 [21–82]
Height (cm, median [range])	173 [147–202]	175 [147–202]	169 [149–196]
Weight (kg, median [range])	79 [45–130]	80 [46–130]	73 [45–124]
BMI (kg/m^2, median [range])	25.4 [17.6–42.5]	25.6 [18.1–42.5]	25.2 [17.6–37.2]
Concomitant therapy			
No gastric acid-suppressive agents	110 (82%)	75 (78%)	35 (90%)
With gastric acid-suppressive agents	25 (18%)	21 (22%)	4 (10%)
Pazopanib dosing			
Pazopanib initial dose per individual (mg, range)	800 (200–800)	800 (200–800)	800 (400–800)
Pazopanib median dose per individual (mg, range)	600 (200–1000)	600 (200–1000)	600 (200–1000)
Pazopanib median treatment days (days, IQR)	120 (63–372)	176 (63–410)	93 (61–192)
Number of individuals with dose reduction occasion (*N*, %)	66/135 (49%)	50/96 (52%)	16/39 (41%)
Number of individuals with dose increase occasion (*N*, %)	51/135 (37%)	39/96 (40%)	12/39 (30%)
Pharmacokinetic data			
Total number of observations (*N*)	460	356	104
Number of trough concentrations (*N*)	326 (70%)	252 (70%)	74 (71%)
Number of observations per patient (*N*, median with IQR)	3 (1–23)	3 (1–23)	2 (1–11)
Median overall pazopanib concentration (mg/L, IQR) ($n = 460$)	29 (2–77)	28 (3–77)	30 (2–75)
Median Trough pazopanib concentration (mg/L, IQR) ($n = 324$)	27 (22–35)	27 (22–34)	27 (21–39)
Median time after last dose (h, IQR)	24 (0.5–166)	24 (0.5–166)	24 (2.5–58)
Median time after start of treatment (days, IQR)	120 (63–372)	177 (63–410)	93 (61–193)
Liver toxicity data ($N = 135$)			
CTCAE grade = 1 (*N*)	55	36	19
CTCAE grade = 2 (*N*)	11	8	3
CTCAE grade ≥ 3 (*N*)	16	13	3
Tumor size (TS) data ($N = 111$)			
Total number of TS observations (*N*)	403	322	81
Median number of TS observations per patient (*N*, IQR)	3 (2–6)	4 (2–6)	2 (1–3)
Median baseline SLD (mm, IQR)	82 (54–134)	79 (50–129)	88 (64–148)
Median SLD during treatment (mm, IQR)	62 (36–111)	53 (33–103)	112 (61–160)

Covariates including pazopanib dose on the day before the toxicity event, pazopanib initial dose, different exposure metrics, age, body weight, sex, and tumor type were tested on the base hazard model. Owing to correlations between dose and exposure metrics, only a first round of covariate selection was performed, and the most significant covariate was selected. $C_{min,ss}$ had the largest dOFV of 8.03 and was selected as covariate. The hazard of developing liver toxicity did not differ between mRCC and STS, as depicted in Supplementary Fig. S5. A $C_{min,ss}$ of ≥ 34 mg/L was identified as the liver toxicity threshold that resulted in a significant increase in hazard (i.e., 3.35-fold hazard increase ($P < 0.01$)) compared with $C_{min,ss} < 34$ mg/L. Details of the hazard ratio fold changes are depicted in Supplementary Table S1 and Supplementary Fig. S7, where it could be observed that the hazard was increased and maintained at high coefficient when $C_{min,ss} \geq 34$ mg/L. The parameter estimates of the final toxicity model are provided in Table 3. The SHAPE parameter indicated the general trend of the hazard: in our analysis, the SHAPE value of −0.012 per day indicated that the hazard decreased from the baseline over time. The survival-based VPC of final toxicity model, as shown in Fig. 1, indicates a significantly lower CTCAE ≥ 2 liver toxicity-free survival when $C_{min,ss} > 34$ mg/L. Hazard-based VPC, which was provided in Supplementary Fig. S8, indicated good alignment between model-predicted hazard and the true hazard.

Table 2 POPPK parameter estimates of pazopanib for the final model for mRCC and STS patients, and results of bootstrap analysis

Parameters	Estimates (RSE) [Shrinkage]	Bootstrap results (median+ 95% CI)
CL/*F* (L/h)	0.497 (7%)	0.490 (0.40–0.57)
V/F (L)	46.1 (19%)	44.6 (32.6–63.0)
Ka (h)	0.976 FIX [24]	0.976 FIX [24]
$F1 = TVF1 * (200/DOSE)^{EXP}$		
TVF_1	1 FIX	1 FIX
EXP	0.42 (12%)	0.43 (0.32–0.57)
IIV_V/F (CV%)	76.5% (16%) [51%]	72.1% (45.5%– 92.7%)
IIV_F1 (CV%)	34.2% (9%) [15%]	34.0% (27.9%– 40.0%)
Proportional error (CV%)	24% (10%)	24% (16%– 29%)
Additive error (mg/L)	4.71 (20%)	4.60 (1.15–7.48)

CL/F apparent clearance, *V/F* volume of distribution, *Ka* absorption rate constant, F_1 bioavailability, *IIV_CL* inter individual variability of clearance, *IIV_V* inter individual variability of volume of distribution, IIV_F_1 inter individual variability of bioavailability

3.4 Exposure–Tumor Size Dynamics Analysis

The visualization of collected SLD data is depicted in Supplementary Fig. S9. For the tumor size dynamics model, the model structure was the same for both tumor types and is shown in Fig. 2 and Eqs. 7–8. The tumor size modeling results, as depicted in Table 4, showed that the tumor growth model accounting for the presence of different subpopulations that have primary resistance and/or acquired resistance could adequately describe the collected SLD data. The introduction of a subpopulation with primary resistance by using a mixture model improved the model fit significantly (27% and 13% for mRCC and STS, dOFV > 3.84), as well as the distribution of ETA on decay rate (KD), with a shift towards a more normal distribution and reduced skewness. For tumor growth rate estimates (KG), first-order apparent growth rate (day^{-1}) was estimated to be 0.0005 for mRCC and 0.0086 for STS. For the KD, a linear decay rate was estimated (0.004 day^{-1} for mRCC and 0.008 day^{-1} for STS), while neither exposure nor dose dependency was identified as significant covariate for any of the tumor types. Acquired resistance rate λ (day^{-1}) was described by an exponential function with time dependency (0.008 for mRCC and 0.0003 for STS). RSE for all estimates were ≤ 30%, except for resistance rate of STS (59%). Detailed diagnostic plots of the final tumor size dynamic model are shown in Fig. 3, and a VPC based on 1000 simulations and considering dropout is presented in Supplementary Fig. S10.

3.5 Model-Based Simulations for Dose Optimization

Model-based simulations of the final models on pazopanib exposure over time, CTCAE ≥ 2 liver toxicity probability over time, and tumor size dynamics over time after pazopanib treatment were performed to compare different pazopanib initial dose regimens. As depicted in Fig. 4, the 800 mg and the 600 mg QD starting dose are anticipated to lead to adequate efficacy, as $C_{min,ss}$ remains above the target threshold of 20.5 mg/L in 76% of the simulated individuals. In contrast, the 800 mg starting dose significantly increased the hazard of developing a liver toxicity event. For both mRCC and STS, no additional exposure or dose dependency was observed (right panel). Tumor sizes highly overlapped for both regimens, regardless of the tumor type. A shiny application was developed in which a randomly collected pazopanib PK sample can be the input, and it will provide the current predicted $C_{min,ss}$ and the $C_{min,ss}$ values for alternative regimens as a reference (Supplementary Fig. S11).

Table 3 Parameter estimates of the final TTE model with a Gompertz distribution

Parameters	Estimates (RSE)	Bootstrap results (median + 95% CI)
Lamda (1/day)	0.0021 (33%)	0.0020 (0.0010, 0.0034)
SHAPE (1/day)	− 0.012 (28%)	− 0.012 (− 0.021, − 0.007)
$C_{min,ss}$ coefficient (coef)$^{*\&}$	1.21 (32%)$^{\&}$	1.30 (0.93, 2.07)

*If C_{min}. ss > 34 mg/L, $h(t)$ = LAMDA * $e^{(*)}$ * $e^{()}$ [=] $^{\&}$: fold change is $e^{(coef)} = 3.35$

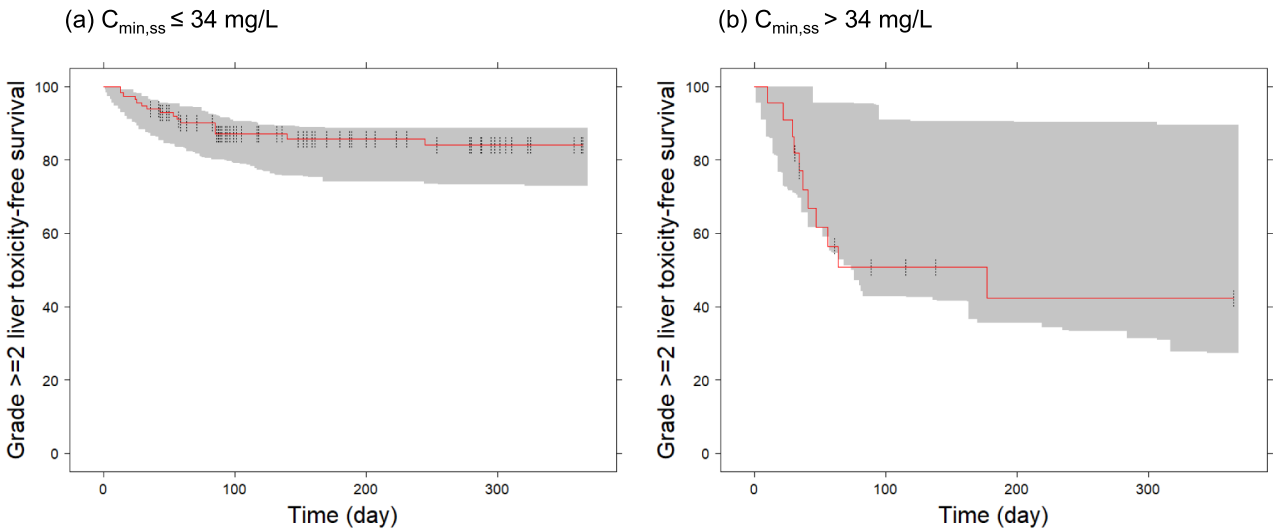

Fig. 1 Survival-based visual predictive check Kaplan–Meier plots of the probability of being free of grade ≥ 2 liver toxicity over a 1-year censoring time, stratified by a $C_{min,ss}$ threshold of 34 mg/L derived from the final liver toxicity model. The solid red lines represent the Kaplan–Meier curve of the observed data and the grey shaded areas represent the 95% prediction intervals. The vertical lines represent censored observations

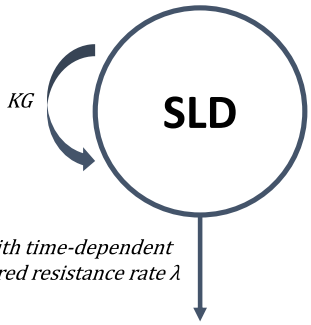

For primary sensitive population (SLD_s):

$$\frac{dSLD\_s}{dt} = KG * SLD\_s - KD * e^{-\lambda t} * SLD\_s \quad (7)$$

For primary resistant population (SLD_r):

$$\frac{dSLD\_r}{dt} = KG * SLD\_r \quad (8)$$

Fig. 2 Final tumor size model structure based on the sum of longest diameters (SLD) for both mRCC and STS. Primary sensitive population (SLD_s) and primary resistant population (SLD_r) were distinguished by implementing a mixture model in NONMEM. SLD_r was assumed to have no drug-induced decay, and therefore, KD was fixed to 0. *KG* growth rate, *KD* decay rate, λ acquired resistance rate

Table 4 Parameter estimates of tumor size dynamics model

Tumor type	mRCC		STS	
	Estimate (RSE%)	Bootstrap (median + 95% CI)	Estimate (RSE%)	Bootstrap (median + 95% CI)
Growth rate KG (day^{-1})	0.0005 (31)	0.0005 (0.0002–0.001)	0.0086 (22)	0.0086 (0.0085–0.0087)
Decay rate KD (day^{-1})	0.004 (15)	0.004 (0.003–0.006)	0.008 (24)	0.0078 (0.0078–0.008)
Acquired resistant rate λ (day^{-1})	0.008 (16)	0.008 (0.006–0.012)	0.0003 (59)	0.0003 (0.0002–0.0004)
Subpopulation of primary resistance (%)	27% (12)	26% (8–50%)	13.4% (8)	14% (10–23%)
Random effects CV% [shrinkage%]				
IIV_KG	130% (18) [27]	125% (77–167%)	0 FIX	–
1IIV_KD	54% (20) [27]	46% (30–64%)	13% (33) [29]	12% (6.7–17.8%)
Residual error (RSE%)				
Propotional error (%)	13.8% (3)	14% (11–17%)	16.6% (18)	17% (0.16–0.17)
Additive error (mm)	1.24 (33)	1.12 (1–1.63)	8.1 (71)	8.2 (8–8.2)

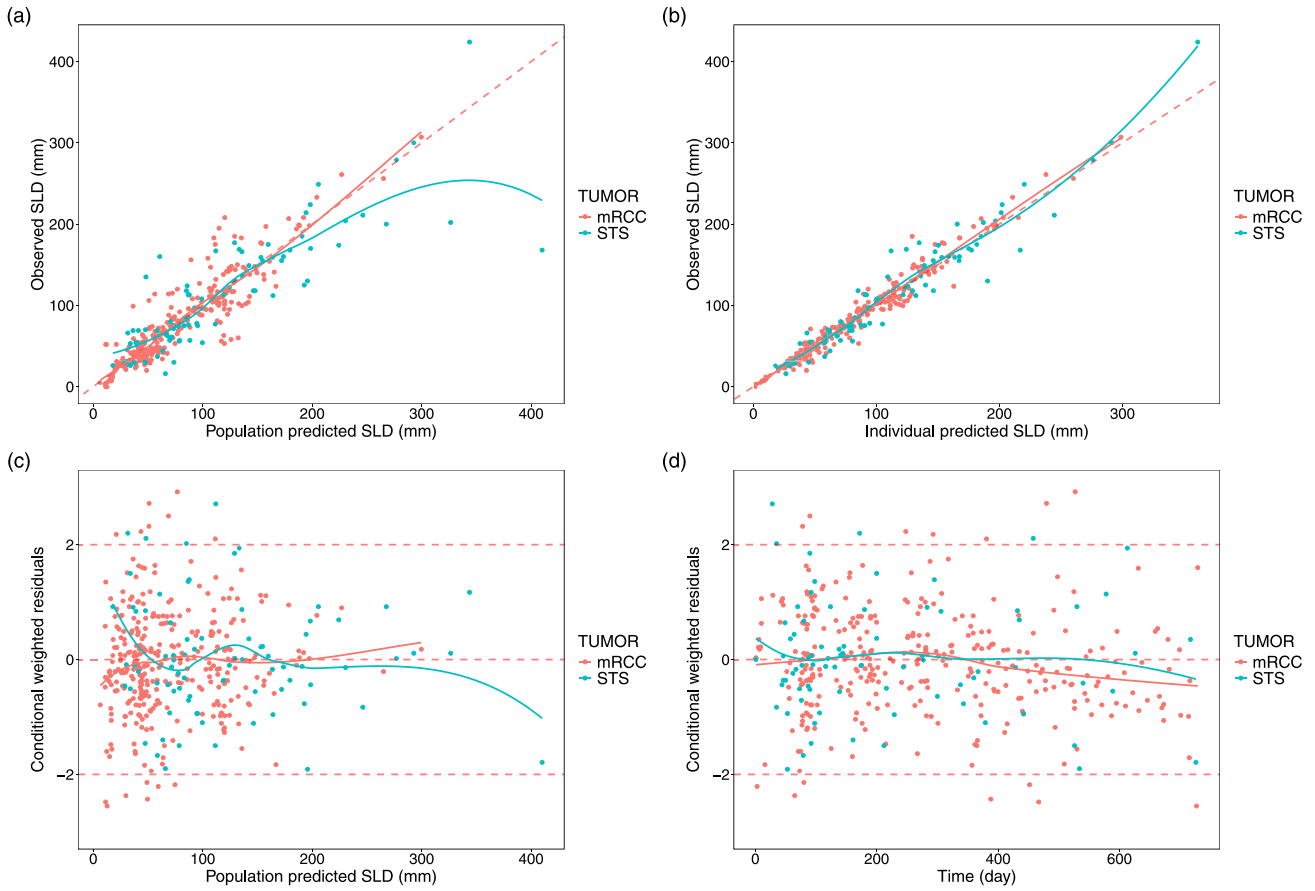

Fig. 3 Goodness-of-fit plots of final TS dynamics model. **a** Population-predicted SLD versus observed SLD; **b** individual predicted SLD versus observed SLD; (3) population-predicted SLD versus conditional weighted residual errors; (4) time after treatment start versus conditional weighted residual errors

4 Discussion

In this study, we performed a comprehensive evaluation of the pazopanib POPPK, exposure–liver toxicity relationship, and exposure–tumor size dynamics of real-world patients with mRCC and STS treated with pazopanib. A one-compartment POPPK model with dose-nonlinearity on F_1 described the data well. In the exposure–liver toxicity analysis, $C_{min,ss}$ was identified as significant covariate and a $C_{min,ss}$ threshold > 34 mg/L indicated a 3.35-fold higher hazard of CTCAE grade ≥ 2 liver toxicity compared with $C_{min,ss}$ ≤ 34 mg/L. Exposure–tumor size dynamic models incorporating tumor heterogeneity were established for both tumor types separately. No additional pazopanib dose or exposure effects on tumor growth were observed in our cohort, with TDM trough samples generally above 20.5 mg/L, which suggests that the current $C_{min,ss}$ target was adequate for both mRCC and STS.

There is ample evidence suggesting that the approved 800 mg QD pazopanib fixed dose is not the optimal initial dose. The approved dose was established using the maximum tolerated dose (MTD), where no dose-limiting toxicities were identified. In addition, only one dose level of 800 mg QD was evaluated in the registration study [27]. According to the US Food and Drug Administration (FDA) registration file [28], the FDA reviewers combined all available patients from the clinical trials [28] and divided the $C_{min,ss}$ into quantiles for a survival analysis. The survival curves of patients with different trough concentration quartile groups overlapped at several points, suggesting the absence of an exposure–response relationship within the exposure range at the 800 mg QD dosing regimen. A logistic regression analysis was performed with registration trial toxicity data [29] and found that the probability of grade 3+ ALT increased with increased pazopanib exposure. This reflects a limitation of the MTD paradigm, which prioritizes a highest-tolerated dose rather than a dose optimized for long-term tolerability and efficacy. The FDA's recent initiative, project OPTIMUS [30], emphasized the importance to achieve an optimal dose by considering multiple factors such as nonclinical data, PK/PD, biomarker, prior knowledge, modeling, and simulation tools rather than only evaluating the MTD in the registration

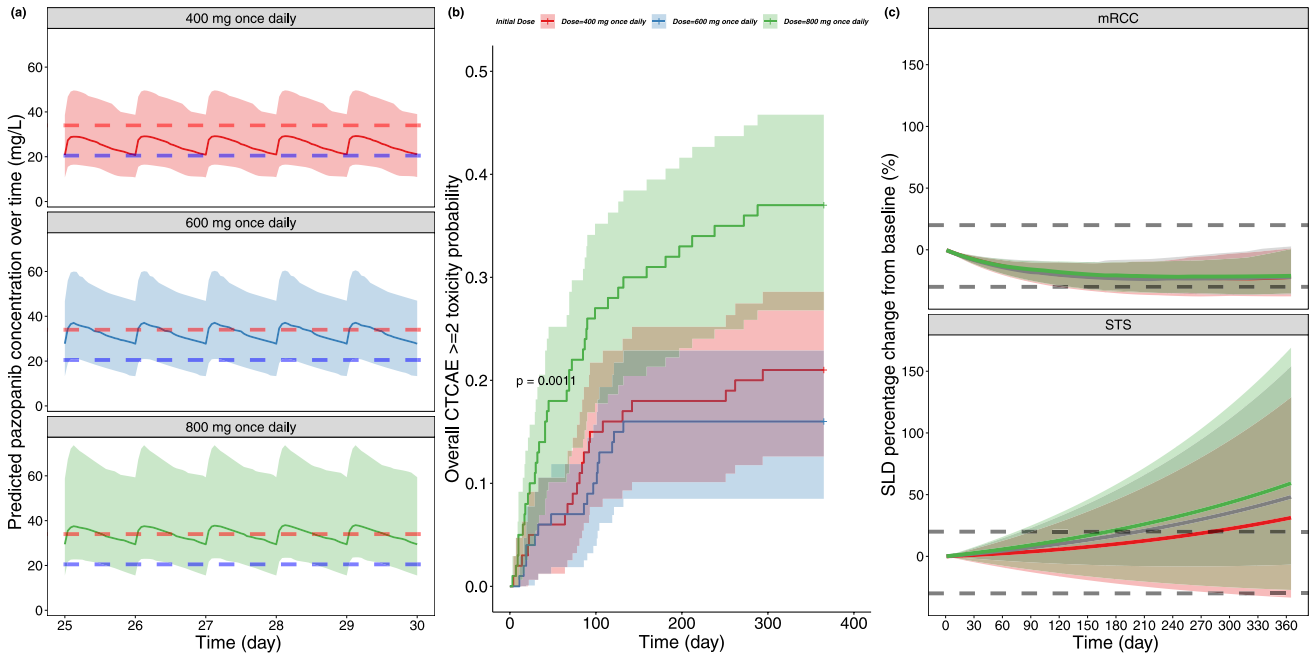

Fig. 4 Model-based simulations of approved 800 mg once daily starting dose (green) and reduced starting doses (600 mg once daily (blue) and 400 mg once daily (red)) with the final pazopanib POPPK model, final liver toxicity model and final tumor size dynamics model. **a** Pazopanib exposure over time of three different dosing regimens, where solid lines represent the median exposure filled with a 90% prediction interval. Blue dashed lines represent the 20.5 mg/L efficacy threshold, and red dashed lines represents the 34 mg/L toxicity threshold. **b** Overall CTCAE ≥ 2 liver toxicity probability over time after pazopanib treatment of three dosing regimens (where solid lines represent the median survival curve filled with a 95% confidence interval). **c** SLD percentage change from baseline over time after pazopanib treatment of three dosing regimens, where solid lines represent the median percentage change of SLD from baseline filled with a 90% prediction interval, for mRCC and STS patients. The grey dashed lines represent the RECIST1.1 criteria of stable disease (SLD shrinkage from − 30 to 20%)

study. In clinical practice, the dose reduction rate (DRR) and related outcomes are reported in several published studies. The DRR ranged from around 40% [31] to 60% [11, 32] in different studies. A statistically significant longer PFS (median 18.2 [95% CI 14.8–21.6] versus 8.2 months [95% CI 6.2–10.2]) and OS (median 30.7 [95% CI 23.6–37.9] versus 19.1 months [95% CI 14.7–23.4]) in patients who underwent dose reductions compared with patients who maintained the starting dose ($P < 0.0001$) was reported in a retrospective study with 179 patients with mRCC who almost exclusively received pazopanib as first-line treatment [33]. Moreover, a food-effect study [34] identified that the intake of 600 mg of pazopanib with breakfast resulted in a bioequivalent exposure established with 800 mg fasted and was preferred over a standard pazopanib dose without food owing to less toxicity.

Previously, several pazopanib POPPK models have been published on the basis of different populations. The first pazopanib POPPK model was retrieved from the FDA registration file [28], where a one-compartment model with dose-dependent KA was established (the FDA model [28]). A more complex two-compartment disposition model with dual absorption, time-dependent, and dose-dependent F_1 was reported by Yu et al. (Yu model [20]) using three clinical trials datasets [20]. Later on, a one-compartment model with a simple absorption model, based on real-world data, was reported by Ozbey et al [26] (the Ozbey model [26]). The typical value of Ka (0.976 h^{-1}) from the Ozbey model [26] was adopted by our study. Different absorption models, with time-dependent or dose-dependent KA and/or F_1, were tested including the complex model from the Yu model [20]. A simplified dose-nonlinearity model, which is a power function, on F_1 could describe our data better than the original complex one due to sparse information on this parameter in our dataset. The estimated CL/F in our analysis is 0.497 L/h, which is the same as reported in the Ozbey model [26] and lower than the estimate reported by the FDA model (0.997 L/h). The V/F estimated from our study is 46 L, which is the same as the FDA model (45 L) and higher than the Ozbey model (22 L). In summary, it seems that the broad range of real-world patients could have lower pazopanib clearance on average (and therefore higher concentrations) than the clinical trial population.

Drug-induced liver toxicity (DILI) is a daily challenge in routine clinical practice [35]. Pazopanib is known for the frequent occurrence of DILI; around 60% of patients

develop moderate liver toxicity that requires dose reduction or dose interruption [33]. Furthermore, 12% of all patients will develop severe liver toxicity that requires dose interruption until remission of symptoms [36]. However, there is no CTCAE ≥ 2 liver toxicity target proposed so far. Previously, a threshold of $C_{min,ss} \leq 50.3$ mg/L for overall grade ≥ 3 toxicity was proposed [13]. Another similar threshold of $C_{min,ss} \leq 46$ mg/L was proposed for overall severe toxicity [7, 12]. A real-world study focusing on liver toxicity tried to investigate the exposure difference between patients that had or did not have CTCAE ≥ 2 liver toxicity [37]. However, pazopanib exposure was comparable in patients with or without liver toxicity (27.7 mg/L versus 28.1 mg/L), and the calculation of $C_{min,ss}$ was based on noncompartmental equations rather than on a modeling approach, which may introduce bias of achieving the "true" $C_{min,ss}$ at the time of the toxicity event [37]. In addition, nonparametric logistic regression was applied in previous research where the time-varying exposure was not taken into consideration [37]. In the current analysis, different exposure metrics were generated by a well-defined POPPK model and parametric TTE modeling approach, which provided an opportunity to simulate different scenarios. A CTCAE ≥ 2 liver toxicity specific threshold of $C_{min,ss} \leq 34$ mg/L was determined on the basis of the evaluation of several thresholds, aiming to improve the continuation of long-term treatment.

Previously, the tumor growth behavior of RCC was investigated by several studies, at both the preclinical and clinical stage, where linear [38, 39], exponential [40], quadratic [41], and logistic [42] models were reported using different datasets. These previously reported growth models were tested in this study. However, the prior knowledge of tumor growth behavior for STS was limited, and only data on an individual level were available [43]. In addition, no study from real-world evidence was reported for mRCC or STS [39, 41, 42]. In the preclinical phase [42], a logistic tumor growth model with an angiogenesis process was implemented where first-order exposure effect (pazopanib area under the curve) was added into the model even though it was unclear whether or how it impacted the model performance. In clinical development [41], a quadratic growth term and a mixture model was implemented to allocate patients in group 1 or group 2. Group 1 accounted for 93 % of the population with subsequent tumor regrowth. Group 2 accounted for 7% of the population, which showed tumor shrinkage without subsequent tumor regrowth. Pazopanib increased the tumor-shrinkage rate in a dose-dependent manner in group 1 patients. Pazopanib 800 mg increased the tumor-shrinkage rate by 267% (95 % CI 215–319%) compared with placebo. In contrast, the tumor-shrinkage rate in group 2 patients was independent of treatment (pazopanib or placebo) and had high IIV and high residual variability. Different from previously published tumor size models for pazopanib, neither dose nor exposure effect were observed to be relevant to tumor shrinkage in our analysis, where the median $C_{min,ss}$ was 26.6 mg/L with IQR 20.6–31.1 mg/L. This indicates that the 20.5 mg/L efficacy threshold is also applicable for patients with STS. Similar evidence could be retrieved from the FDA clinical pharmacology report of pazopanib [28]. The FDA reviewers combined all available patients from the trials [28] and divided the $C_{min,ss}$ into quantiles for survival analysis. The survival curves of patients with different trough concentration quartile groups overlapped at several points, indicating the absence of an exposure–response relationship with the 800 mg QD dosing regimen.

The ultimate goal of this comprehensive model-based analysis is to employ the results for pazopanib MIPD in routine practice. MIPD has been widely used to optimize the dosing schedule of antibiotics to ensure drug exposure over minimal inhibitory concentrations (MIC) [44]; however, there is still only limited application in oncology. Previously, case studies have proven that MIPD can improve the initial dose of imatinib [45] and reduce vincristine-induced peripheral neuropathy in pediatric patients [46]. Recently, Le Loudec et al. developed the mapbayr R package [25], which aims to perform maximum a posteriori Bayesian estimation in R from any POPPK model. On the basis of the pazopanib MIPD shiny example developed by Le Loudec et al., we replaced the model with our POPPK model that could be more representative for a real-world population and introduced the threshold of 20.5 mg/L $\leq C_{min,ss} \leq$ 34 mg/L for both cancer populations. The shiny application can generate the dose-adjustment recommendation from extrapolating randomly taken samples to trough levels. The details of our updated pazopanib MIPD shiny application can be found at https://github.com/tanzy1995/pazopanib-MIPD. There are commercial MIPD tools available that could incorporate PK models such as the one provided in our manuscript. However, the application of MIPD tools such as the shiny interface provided in this manuscript in routine clinical practice faces significant challenges. These challenges include the requirement of a lot of (legal) documentation, validation, and testing for every change that is made to the tool, even if it is used solely in an ISO 15189 laboratory environment. These tools in general, while promising for improving individualized dosing, currently occupy a regulatory oversight where a clear framework is formally required to label them as medical devices [47]. This ambiguity complicates their widespread adoption, especially considering the potential risk of using these tools to prescribe off-label dose, which could lead to safety concerns [47, 48]. Additionally, the integration of MIPD into clinical workflows requires overcoming operational barriers, such as the need for real-time data input, model validation, and proper healthcare professional education [48, 49]. Collaborative efforts among diverse stakeholders for MIPD tool regulation (clear regulation

pathway), model validation, education, and implementation are warranted [47–49].

The present study has several limitations. First, owing to the rare nature of STS, only a limited number of data could be retrieved for the tumor size data of patients with STS. In addition, no prior knowledge on the tumor growth behavior, killing effect, or resistance could be found for STS. In that case, the KG rate, KD rate, and resistance rate of STS were all interpreted as "apparent" constant rate rather than a "real" constant rate. In our analysis, we used baseline tumor size as a regressor rather than estimating it to have stable estimation. However, this study is the first that investigated the relationships between PK, toxicity, and tumor size dynamics of pazopanib not only in mRCC but also in STS in a real-world setting. Second, owing to the fact that the data in our analysis were collected from real-world practice, which included TDM, most of the included patients were well managed according to the current pazopanib TDM guidelines [50–52]; therefore, the median predicted $C_{min,ss}$ was 26.6 mg/L with an IQR of 20.6–31 mg/L, which was beyond the established efficacy threshold. Potential bias could have been introduced when the pazopanib exposure or dose effect on tumor size dynamics was investigated, with pazopanib $C_{min,ss} < 20.5$ mg/L being evaluated in only 16 out of 111 patients (14%). Finally, only moderate liver toxicity was evaluated in the toxicity analysis owing to the limited number of severe events that occurred in our cohort. Therefore, further analysis with more extensive data is warranted to validate the current liver toxicity threshold and to explore the correlation between pazopanib dose/exposure and severe (CTCAE grade ≥ 3) liver toxicity. In addition, other frequent toxicities such as diarrhea, increased MAP, and stomatitis should also be considered in future studies.

5 Conclusions

The pazopanib exposure–liver toxicity model indicates that a $C_{min,ss} > 34$ mg/L significantly increases the risk of developing CTCAE ≥ 2 liver toxicity for mRCC and STS. In contrast, no clear effect of exposure was observed in the exposure–tumor size dynamics model for both tumor types within our cohort, with a median $C_{min,ss}$ of 26.6 mg/L and an IQR of 20.6–31.1 mg/L. A decreased pazopanib initial dose of 600 mg QD fasted, followed by routine MIPD practice once every 2–3 months aiming at a $C_{min,ss}$ target of 20–34 mg/L with the developed POPPK model could potentially improve the balance between efficacy and treatment toxicity.

Supplementary Information The online version contains supplementary material available at https://doi.org/10.1007/s40262-025-01504-5.

Acknowledgements The authors acknowledge Max Kramer and Mike Volwater for their contribution to this work.

Declarations

Funding The work of Zhiyuan Tan was supported by the China Scholarship Council (202108310028).

Conflict of Interest Catherijne A.J. Knibbe and Dirk Jan A.R. Moes are Editorial Board members of Clinical Pharmacokinetics. Catherijne A.J. Knibbe and Dirk Jan A.R. Moes were not involved in the selection of peer reviewers for the manuscript nor any of the subsequent editorial decisions.

Code and Data Availability Data are available from the corresponding author upon reasonable request. All the model codes were provided in supplementary materials.

Ethics Approval This study was conducted in accordance with Good Clinical Practice guidelines and the Declaration of Helsinki. The protocol was approved by the institutional review board (IRB) at the Scientific Committee of the Department of Medical Oncology, Medical Ethics Review Committee Leiden/Den Haag/Delft. As retrospective data from routine clinical care were used, a waiver was granted for the requirement of informed consent by the IRB.

Consent to Participate/Consent for Publication As retrospective data from routine clinical care were used, a waiver was granted for the requirement of informed consent by the IRB.

Author Contributions Z.T., S.V., A.Y., C.A.J.K., and D.J.A.R.M. contributed to the research design, performed research, analyzed data, and wrote the manuscript. A.R., A.J.G., and T.H. treated patients and reviewed and revised the manuscript.

References

1. Miyamoto S, Kakutani S, Sato Y, Hanashi A, Kinoshita Y, Ishikawa A. Drug review: pazopanib. Jpn J Clin Oncol. 2018;48(6):503–13.
2. Sternberg CN, Hawkins RE, Wagstaff J, Salman P, Mardiak J, Barrios CH, Zarba JJ, Gladkov OA, Lee E, Szczylik C, McCann L, Rubin SD, Chen M, Davis ID. A randomised, double-blind phase III study of pazopanib in patients with advanced and/or metastatic renal cell carcinoma: final overall survival results and safety update. Eur J Cancer (Oxford, England: 1990). 2013;49(6):1287–96.
3. Escudier B, Porta C, Schmidinger M, Rioux-Leclercq N, Bex A, Khoo V, Grünwald V, Gillessen S, Horwich A. Renal cell carcinoma: ESMO Clinical Practice Guidelines for diagnosis, treatment and follow-up. Ann Oncol. 2019;30(5):706–20.

4. Ljungberg B, Albiges L, Abu-Ghanem Y, Bensalah K, Dabestani S, Fernández-Pello S, Giles RH, Hofmann F, Hora M, Kuczyk MA, Kuusk T, Lam TB, Marconi L, Merseburger AS, Powles T, Staehler M, Tahbaz R, Volpe A, Bex A. European Association of Urology guidelines on renal cell carcinoma: the 2019 update. Eur Urol. 2019;75(5):799–810.
5. van der Graaf WT, Blay JY, Chawla SP, Kim DW, Bui-Nguyen B, Casali PG, Schöffski P, Aglietta M, Staddon AP, Beppu Y, Le Cesne A, Gelderblom H, Judson IR, Araki N, Ouali M, Marreaud S, Hodge R, Dewji MR, Coens C, Demetri GD, Fletcher CD, Dei Tos AP, Hohenberger P. Pazopanib for metastatic soft-tissue sarcoma (PALETTE): a randomised, double-blind, placebo-controlled phase 3 trial. Lancet (London, England). 2012;379(9829):1879–86.
6. Nguyen DT, Shayahi S. Pazopanib: approval for soft-tissue sarcoma. J Adv Pract Oncol. 2013;4(1):53–7.
7. Suttle AB, Ball HA, Molimard M, Hutson TE, Carpenter C, Rajagopalan D, Lin Y, Swann S, Amado R, Pandite L. Relationships between pazopanib exposure and clinical safety and efficacy in patients with advanced renal cell carcinoma. Br J Cancer. 2014;111(10):1909–16.
8. Mueller-Schoell A, Groenland SL, Scherf-Clavel O, van Dyk M, Huisinga W, Michelet R, Jaehde U, Steeghs N, Huitema ADR, Kloft C. Therapeutic drug monitoring of oral targeted antineoplastic drugs. Eur J Clin Pharmacol. 2020.
9. Sternberg CN, Davis ID, Mardiak J, Szczylik C, Lee E, Wagstaff J, Barrios CH, Salman P, Gladkov OA, Kavina A, Zarbá JJ, Chen M, McCann L, Pandite L, Roychowdhury DF, Hawkins RE. Pazopanib in locally advanced or metastatic renal cell carcinoma: results of a randomized phase III trial. J Clin Oncol. 2010;28(6):1061–8.
10. Motzer RJ, Hutson TE, Cella D, Reeves J, Hawkins R, Guo J, Nathan P, Staehler M, de Souza P, Merchan JR, Boleti E, Fife K, Jin J, Jones R, Uemura H, De Giorgi U, Harmenberg U, Wang J, Sternberg CN, Deen K, McCann L, Hackshaw MD, Crescenzo R, Pandite LN, Choueiri TK. Pazopanib versus sunitinib in metastatic renal-cell carcinoma. N Eng J Med. 2013;369(8):722–31.
11. Gaillard V, Lhuillier A, Bigot C, Pierard L, Trensz P, Burgy M, Schuster C, Malouf G, Fritsch A, Lang H, Tricard T, Borchiellini D, Geoffrois L, Barthelemy P. Impact of the app-based and nurse-led supportive care program AKO@dom on dose intensity of oral-targeted therapies in patients with metastatic renal cell cancer: a multicentric observational retrospective study. Support Care Cancer. 2022;30(8):6583–91.
12 Lin Y, Ball HA, Suttle B, Mehmud F, Amado RG, Hutson TE, Pandite LN. Relationship between plasma pazopanib concentration and incidence of adverse events in renal cell carcinoma. J Clin Oncol. 2011;29(7_suppl):345–345.
13. Noda S, Yoshida T, Hira D, Murai R, Tomita K, Tsuru T, Kageyama S, Kawauchi A, Ikeda Y, Morita SY, Terada T. Exploratory investigation of target pazopanib concentration range for patients with renal cell carcinoma. Clin Genitourin Cancer. 2019;17(2):e306–13.
14. Minichmayr IK, Dreesen E, Centanni M, Wang Z, Hoffert Y, Friberg LE, Wicha SG. Model-informed precision dosing: state of the art and future perspectives. Adv Drug Deliv Rev. 2024;215:115421.
15. Escudero-Ortiz V, Domínguez-Leñero V, Catalán-Latorre A, Rebollo-Liceaga J, Sureda M. Relevance of therapeutic drug monitoring of tyrosine kinase inhibitors in routine clinical practice: a pilot Study Pharmaceutics [Online], 2022.
16. Gotta V, Widmer N, Decosterd LA, Chalandon Y, Heim D, Gregor M, Benz R, Leoncini-Franscini L, Baerlocher GM, Duchosal MA, Csajka C, Buclin T. Clinical usefulness of therapeutic concentration monitoring for imatinib dosage individualization: results from a randomized controlled trial. Cancer Chemother Pharmacol. 2014;74(6):1307–19.
17. van Erp NP, de Wit D, Guchelaar HJ, Gelderblom H, Hessing TJ, Hartigh J. A validated assay for the simultaneous quantification of six tyrosine kinase inhibitors and two active metabolites in human serum using liquid chromatography coupled with tandem mass spectrometry. J Chromatogr. 2013;937:33–43.
18. SERVICES, U. S. D. O. H. A. H. Common Terminology Criteria for Adverse Events (CTCAE) v5.0. https://ctep.cancer.gov/protocoldevelopment/electronic_applications/ctc.htm#ctc_50. Accessed 27 Nov 2017.
19. Schwartz LH, Litière S, de Vries E, Ford R, Gwyther S, Mandrekar S, Shankar L, Bogaerts J, Chen A, Dancey J, Hayes W, Hodi FS, Hoekstra OS, Huang EP, Lin N, Liu Y, Therasse P, Wolchok JD, Seymour L. RECIST 1.1—Update and clarification: from the RECIST committee. Eur J Cancer (Oxford, England : 1990). 2016;62:132–7.
20. Yu H, van Erp N, Bins S, Mathijssen RH, Schellens JH, Beijnen JH, Steeghs N, Huitema AD. Development of a pharmacokinetic model to describe the complex pharmacokinetics of pazopanib in cancer patients. Clin Pharmacokinet. 2017;56(3):293–303.
21. Mir O, Touati N, Lia M, Litière S, Le Cesne A, Sleijfer S, Blay JY, Leahy M, Young R, Mathijssen RHJ, Van Erp NP, Gelderblom H, Van der Graaf WT, Gronchi A. Impact of concomitant administration of gastric acid-suppressive agents and pazopanib on outcomes in soft-tissue sarcoma patients treated within the EORTC 62043/62072 trials. Clin Cancer Res. 2019;25(5):1479–85.
22. Bergstrand M, Hooker AC, Wallin JE, Karlsson MO. Prediction-corrected visual predictive checks for diagnosing nonlinear mixed-effects models. AAPS J. 2011;13(2):143–51.
23 Van Wijk RC, Simonsson USH. Finding the right hazard function for time-to-event modeling: a tutorial and shiny application. CPT Pharmacomet Syst Pharmacol. 2022;11(8):991–1001.
24. Huh Y, Hutmacher MM. Application of a hazard-based visual predictive check to evaluate parametric hazard models. J Pharmacokinet Pharmacodynam. 2016;43(1):57–71.
25. Le Louedec F, Puisset F, Thomas F, Chatelut É, White-Koning M. Easy and reliable maximum a posteriori Bayesian estimation of pharmacokinetic parameters with the open-source R package mapbayr. CPT Pharmacomet Syst Pharmacol. 2021;10(10):1208–20.
26. Ozbey AC, Combarel D, Poinsignon V, Lovera C, Saada E, Mir O, Paci A. Population pharmacokinetic analysis of pazopanib in patients and determination of target AUC. Pharmaceuticals (Basel, Switzerland). 2021;14 (9).
27. Hurwitz HI, Dowlati A, Saini S, Savage S, Suttle AB, Gibson DM, Hodge JP, Merkle EM, Pandite L. Phase I trial of pazopanib in patients with advanced cancer. Clin Cancer Res. 2009;15(12):4220–7.
28. RESEARCH, C. F. D. E. A., Votrient (pazopanib) tablets. Clin Pharmacol Bipharmaceut Rev. 2009.
29. Motzer RJ, Hutson TE, Cella D, Reeves J, Hawkins R, Guo J, Nathan P, Staehler M, de Souza P, Merchan JR, Boleti E, Fife K, Jin J, Jones R, Uemura H, De Giorgi U, Harmenberg U, Wang J, Sternberg CN, Deen K, McCann L, Hackshaw MD, Crescenzo R, Pandite LN, Choueiri TK. Pazopanib versus sunitinib in metastatic renal-cell carcinoma. New Eng J Med. 2013;369(8):722–31.
30. Administration, F. a. D., Optimizing the dosage of human prescription drugs and biological products for the treatment of oncologic diseases, guidance for industry. *Biologics*, U. S. D. o. H. a. H. S. F. a. D. A. O. C. o. E. O. C. f. D. E. a. R. C. C. f., Ed. 2024.
31. Shah AY, Kotecha RR, Lemke EA, Chandramohan A, Chaim JL, Msaouel P, Xiao L, Gao J, Campbell MT, Zurita AJ, Wang J, Corn PG, Jonasch E, Motzer RJ, Sharma P, Voss MH, Tannir NM. Outcomes of patients with metastatic clear-cell renal cell carcinoma treated with second-line VEGFR-TKI after first-line

immune checkpoint inhibitors. Eur J Cancer (Oxford, England : 1990). 2019;114:67–75.
32. Johnston H, Deal AM, Morgan KP, Patel B, Milowsky MI, Rose TL. Dose intensity in real-world patients with metastatic renal cell carcinoma taking vascular endothelial growth factor receptor tyrosine kinase inhibitors. Clin Genitourin Cancer. 2023;21(3):357–65.
33. Corianò M, Giannarelli D, Scartabellati G, De Giorgi U, Brighi N, Fornarini G, Tommasi C, Giudice GC, Rebuzzi SE, Puglisi S, Caffo O, Kinspergher S, Mennitto A, Cattrini C, Santoni M, Verzoni E, Rametta A, Stellato M, Malgeri A, Roviello G, Brunelli M, Signori A, Banna GL, Buti S. Tailoring treatment with cabozantinib or pazopanib in patients with metastatic renal cell carcinoma: does it affect outcome? Exp Review Anticancer Ther. 2023;23(5):545–54.
34. Lubberman FJE, Gelderblom H, Hamberg P, Vervenne WL, Mulder SF, Jansman FGA, Colbers A, van der Graaf WTA, Burger DM, Luelmo S, Moes DJAR, van Herpen CML, van Erp NP. The effect of using pazopanib with food vs. fasted on pharmacokinetics, patient safety, and preference (DIET Study). Clin Pharmacol Ther. 2019;106(5):1076–82.
35. Rini BI, Plimack ER, Stus V, Gafanov R, Hawkins R, Nosov D, Pouliot F, Alekseev B, Soulières D, Melichar B, Vynnychenko I, Kryzhanivska A, Bondarenko I, Azevedo SJ, Borchiellini D, Szczylik C, Markus M, McDermott RS, Bedke J, Tartas S, Chang YH, Tamada S, Shou Q, Perini RF, Chen M, Atkins MB, Powles T. Pembrolizumab plus axitinib versus sunitinib for advanced renal-cell carcinoma. New Eng J Med. 2019;380(12):1116–27.
36. Pick AM, Nystrom KK. Pazopanib for the treatment of metastatic renal cell carcinoma. Clin Therapeut. 2012;34(3):511–20.
37. Westerdijk K, Krens SD, Steeghs N, van der Graaf WTA, Tjwa E, Westdorp H, Desar IME, van Erp NP. Real-world data on the management of pazopanib-induced liver toxicity in routine care of renal cell cancer and soft tissue sarcoma patients. Cancer Chemother Pharmacol. 2024;93(4):353–64.
38. Stein A, Wang W, Carter AA, Chiparus O, Hollaender N, Kim H, Motzer RJ, Sarr C. Dynamic tumor modeling of the dose-response relationship for everolimus in metastatic renal cell carcinoma using data from the phase 3 RECORD-1 trial. BMC Cancer. 2012;12:311.
39. Maitland ML, Wu K, Sharma MR, Jin Y, Kang SP, Stadler WM, Karrison TG, Ratain MJ, Bies RR. Estimation of renal cell carcinoma treatment effects from disease progression modeling. Cancer Pharmacol Ther. 2013;93(4):345–51.
40. Claret L, Mercier F, Houk BE, Milligan PA, Bruno R. Modeling and simulations relating overall survival to tumor growth inhibition in renal cell carcinoma patients. Cancer Chemother Pharmacol. 2015;76(3):567–73.
41. Bonate PL, Suttle AB. Modeling tumor growth kinetics after treatment with pazopanib or placebo in patients with renal cell carcinoma. Cancer Chemother Pharmacol. 2013;72(1):231–40.
42. Ouerdani A, Struemper H, Suttle AB, Ouellet D, Ribba B. Preclinical modeling of tumor growth and angiogenesis inhibition to describe pazopanib clinical effects in renal cell carcinoma. CPT Pharmacomet Syst Pharmacol. 2015;4(11):660–8.
43. Spratt JR., JS, The rates of growth of skeletal sarcomas. Cancer. 1965;18(1): 14-24.
44. Wicha SG, Märtson AG, Nielsen EI, Koch BCP, Friberg LE, Alffenaar JW, Minichmayr IK. From therapeutic drug monitoring to model-informed precision dosing for antibiotics. Cancer Pharmacol Ther. 2021;109(4):928–41.
45. Goutelle S, Guidi, M, Gotta V, Csajka C, Buclin T, Widmer N. From personalized to precision medicine in oncology: a model-based dosing approach to optimize achievement of imatinib target exposure. Pharmaceutics. 2023;15(4).
46. Centanni M, van de Velde ME, Uittenboogaard A, Kaspers GJL, Karlsson MO, Friberg LE. Model-informed precision dosing to reduce vincristine-induced peripheral neuropathy in pediatric patients: a pharmacokinetic and pharmacodynamic modeling and simulation analysis. Clin Pharmacokinet. 2024;63(2):197–209.
47. Keizer RJ, Dvergsten E, Kolacevski A, Black A, Karovic S, Goswami S, Maitland ML. Get Real: Integration of real-world data to improve patient care. Clin Pharmacol Ther. 2020;107(4):722–5.
48. Dibbets AC, Koldeweij C, Osinga EP, Scheepers HCJ, de Wildt SN. Barriers and facilitators for bringing model-informed precision dosing to the patient's bedside: a systematic review. Clin Pharmacol Ther. 2025;117(3):633–45.
49. Darwich AS, Ogungbenro K, Vinks AA, Powell JR, Reny J-L, Marsousi N, Daali Y, Fairman D, Cook J, Lesko LJ, McCune JS, Knibbe CAJ, de Wildt SN, Leeder JS, Neely M, Zuppa AF, Vicini P, Aarons L, Johnson TN, Boiani J, Rostami-Hodjegan A. Why has model-informed precision dosing not yet become common clinical reality? Lessons from the past and a roadmap for the future. Clin Pharmacol Ther. 2017;101(5):646–56.
50. Henriksen JN, Andersen CU, Fristrup N. Therapeutic drug monitoring for tyrosine kinase inhibitors in metastatic renal cell carcinoma. Clin Genitourin Cancer. 2024;22(3): 102064.
51. Mueller-Schoell A, Groenland SL, Scherf-Clavel O, van Dyk M, Huisinga W, Michelet R, Jaehde U, Steeghs N, Huitema ADR, Kloft C. Therapeutic drug monitoring of oral targeted antineoplastic drugs. Eur J Clin Pharmacol. 2021;77(4):441–64.
52. Westerdijk K, Desar IME, Steeghs N, van der Graaf WTA, van Erp NP. Imatinib, sunitinib and pazopanib: from flat-fixed dosing towards a pharmacokinetically guided personalized dose. Br J Clin Pharmacol. 2020;86(2):258–73.